THE NATURE OF STRONG WIND EVENTS IN THE NORTHERN GULF OF ALASKA AND PRINCE WILLIAM SOUND.

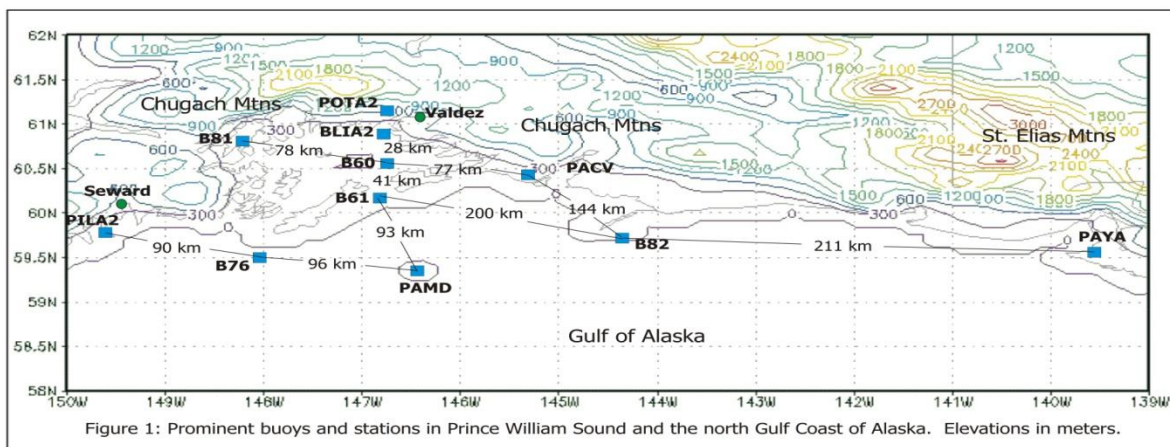**John Papineau, NWS, Anchorage, Alaska**

Introduction:

Moderate to strong winds (gale force) are a common occurrence along the northern coastal zone of the Gulf of Alaska during the cooler months of the year. The region extending from the southern Kenai Peninsula eastward through Prince William Sound (PWS) and on to Yakutat Bay is backed by a nearly continuous arc of steep mountains (Figure 1). These mountains impeded northward moving air masses that might otherwise propagate into southern Alaska. Since the Gulf of Alaska is a region of intense storm generation, the interaction of fronts, troughs, waves and warm air masses with the steep terrain is to be expected to occur on a frequent basis. Strong winds (>20 ms^{-1}) represent a hazard to the marine and aviation users who live or transit the area. For example, oil tankers which are loaded at Valdez, the terminus of the Alaska oil pipeline, must transit PWS before entering the Gulf of Alaska enroute to southern markets. Strong winds, especially east wind events which flow parallel to the terrain, can be a hazard to ships and boats attempting to navigate through PWS. These events are also notable because almost every event is accompanied by heavy precipitation, low visibility, and high seas.

Fortunately a number of National Buoy Data Center (NBDC) buoys and C-man stations have been established over the past decade, allowing the marine users and forecasters to monitor real-time conditions, but also allows researchers the opportunity to investigate the characteristics and frequency of these events. The northern Gulf of Alaska is unique compared to other regions of the globe that experience coastal/barrier wind jets in that cold air over the state can play a role as well. The interplay being the arctic airmass over land and the relatively warmer air over the gulf can lead to a variety of jet formations as documented by Loescher *et al* (2006) and Colle *et al* (2006). In the immediate coastal zone a dome of cold stable air may act to 'shield' the area from strong winds, while in other circumstances the outflow of cold air from the numerous bays, passes and gaps in the coastal mountains can be an important source of mass for what Loescher *et al* (2006) have labeled hybrid jets.   The complete structure of these jets can be seen in Figures 2 and 3 which are SAR images of two strong E-SE wind events.

The barrier formed by the Kenai, Chugach, and St. Elias Mountains range in height from 1000-4000 m, the highest peaks along this particular stretch of coastline are located directly north of PWS. From the Kenai Peninsula (150°W) to eastern PWS (146°W) the mountains extend to the waters edge; further east there is a 15-30 km coastal plain which contains isolated mountains that are generally lower than 1000 m.   As will be demonstrated in this paper, the orientations of most of the fronts that move through the region tend to parallel the arc (NW-SE) of the coastal mountains. Prince William Sound which is the hub of commercial and recreational marine users is separated from the Gulf of Alaska by Hinchinbrook and Montague Islands. These islands are capped by mountains that range up to 900 m in height. The terrain immediately surrounding PWS is the epitome of complex terrain; the sounds' numerous fjords and bays act as gaps through which the already strong winds may undergo further acceleration.

Figure 1: Prominent buoys and stations in Prince William Sound and the north Gulf Coast of Alaska. Elevations in meters.

The goal of this study is too investigate the nature of strong wind events that occur along northern coast of the Gulf of Alaska including Prince William Sound. There are two fundamental types of events: 1) East to southeast coastal jets which are linked to frontal passage; 2) Northerly cold air drainage jets which result from the accumulation of deep cold air over the state of Alaska. This study will utilize SAR imagery as well as surface observations from buoys, C-Man stations, and ASOS . Note that all three types of instrument packages have different wind speed averaging routines. In addition, several events have been simulated using the WRF model in order to investigate various dynamic aspects. After a brief literature review this paper will consider coastal jet cases using surface observations followed by some highlights from WRF simulations. This is followed by a overview of strong northerly jets and then the a conceptual model is offered.

Previous Studies:

The study of strong barrier-parallel winds which have been labeled as either a barrier (BJ) or coastal jet (CJ) began in earnest in the 1970s. A broad range of terrain types have been investigated and a number of field projects have been conducted over the succeeding decades. The 'classic' jet as revealed by Parish (1982) is the product of intense and sustained blocking as very stable air is not capable of flowing over moderate to high mountain barrier. The barrier can be located directly along the coast or the interior of a continent; in either case the fundamentals are unchanged.

In a scale analysis of coastal winds along Vancouver Island Overland & Bond (1995) suggest that when blocking by the terrain is complete (B<1, where B is the Burger number= (hN/Lf); where h is the barrier height, N is the static stability, L is the barrier half-width, and f is the Coriolis parameter) the - barrier -parallel acceleration of the winds above the upstream speed (U) is on the order of U itself.

Doyle (1997) used the COAMPS model to investigate the nature of a mid-winter land falling front(s) along the central California coast. He concludes that the shallow depth of the front, large static stability ahead of the front as well as the steep coastal topography produced the observed low-level mountain-parallel pressure perturbations which in turn enhanced the frontal jet. Li and Chen (1997) studied barrier jet formation off the west coast of Taiwan and found that the strongest jets occur in association with pre-frontal low-level jets (LLJ) located off the southeast coast of China. The barrier jet (BJ) weakens and disappears once the front passes over Taiwan.
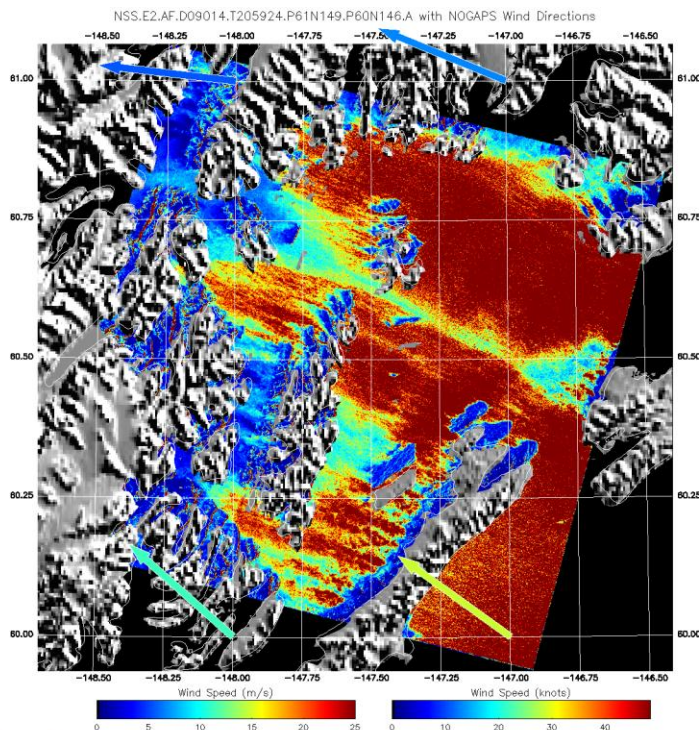

Figure 2: SAR imagery valid at 2059Z on January 14, 2009. Notice the wind streaks to the lee of the various topographic features. B61= E 15 m/s, B60=E 16 m/s, BLIA2= SE 16 m/s, PACV=E-SE 8 m/s.

Braun *et al* (1999) studied the retardation of frontal movement by the coastal mountains using a simplified 2-D model and a highly idealized broad plateau for terrain. Their primary conclusion is that the barrier -parallel (windward base of plateau) flow is a product of both a coastal jet and barrier jet, the latter being a result of upstream blocking by the terrain. They also note a positive correlation between barrier height and strength of the resulting barrier jet.

Colle et al (2002) modeled a cold front that approached the Coast Range of Oregon and northern California. It was found that frontal characteristics (thermal, rain, winds) were intensified as the front moved within 80 km of the coast, in accord with aircraft observations. The authors also found that phase changes and the subsequent warming/cooling of the lower troposphere played an important role in frontogenesis. However, increased blocking for example enhanced precipitation amounts but tended to weaken the thermal gradient and winds. In addition, they conclude that the interaction of a front with variable coastal topography can generate a broad spectrum of local/regional responses in the lower troposphere.

Specific to Alaska, Overland & Bond (1993) have documented a case in which a post-frontal pressure surge developed and subsequently propagate along the coast generating low-level wind speeds well in excess of what one might expect under typical conditions. They suggest that the pronounced pressure surge was generated by the cooling of stable air as it attempted to ascend the steep terrain of Southeast, Alaska. Although detail analysis of this case was not possible, the pressure surge had characteristics that were shared by solitary Kelvin waves.

Using SAR imagery Loescher *et al* (2006) were able to classify northern Gulf of Alaska barrier jet cases into four groups: classical, hybrid, variable and shock. Classical events occur with onshore ambient flow is unable to rise above the coastal mountains. As a result a barrier-parallel pressure gradient develops which helps accelerate the winds above their ambient speeds. Hybrid jets differ from classical jets in that cold air which flows through gaps and passes in the coastal mountains and helps generate

ageostrophic pressure gradients. The authors found that some jets have an "irregular breaks between segmented areas of high wind speed" (Loescher p.442), they labeled these as variable jets. Shock jets in turn are characterized by an abrupt upstream wind speed boundary where the speeds differ by a factor of two or three over horizontal distances of 10 to 20 km.

Figure 3: SAR imagery valid at 0332Z on December 21, 1999. The winds at PACV= E 9 m/s, BLIA2=NE 5 m/s, B60=E-SE 19 m/s, B61=E-SE 16 m/s, PAMD=S 12 m/s, PILA2= NW-N 7 m/s.
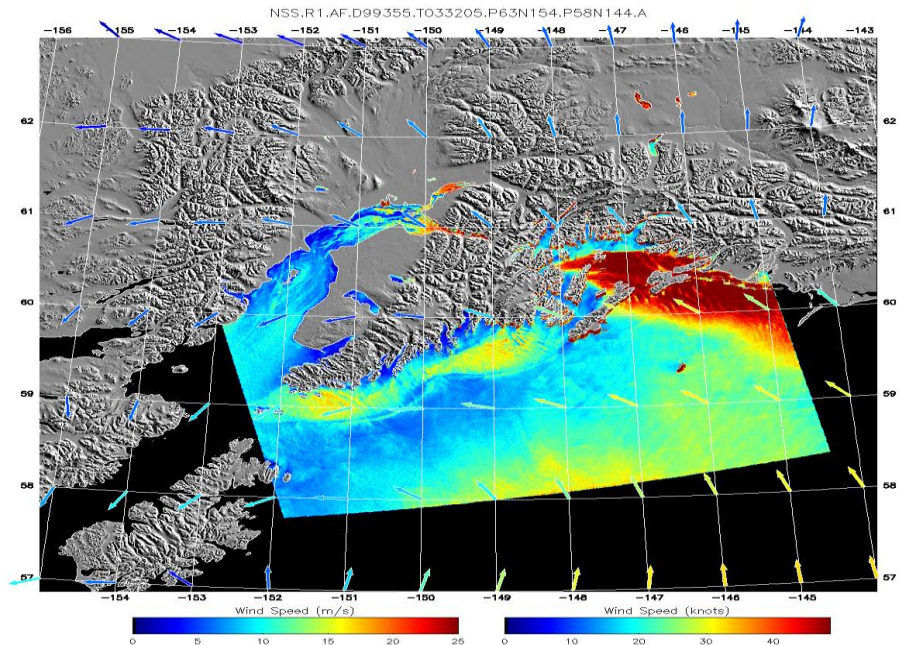
Colle *et al* (2006) in a companion paper used NCEP reanalysis and limited sounding data to investigate the synoptic scale structure of these four types of barrier jets. Some of the primary results are that variable jets have weaker low-level stability profiles when compared to the other types of jets. In addition, shock jets exhibit significant 850 mb cold anomalies over the interior of Alaska and northwest Canada while variable and shock jets typically are associated with reduced upper-level ridging over the interior. Olson et al (2007) were able to investigate two jets that developed along the Fairweather Range using aircraft flights and MM5; the second event was classified as a hybrid jet. The important conclusion of this study is that outflow of cold arctic air through gaps in the terrain can at times be an important source of mass in CJ and in addition generate various localized dynamic 'anomalies' (when compared to the classical events).

Case Studies:

As note in the introduction the terrain that borders the northern Gulf of Alaska varies in height (h)and width (L), in order to establish the hydrodynamic nature of the winds discussed in this paper the Burger (B) number is estimated for a range of values for h and L. With $B=(hN)/(Lf)$, and h=1000-2000 m, L=30-60 km, N=0.013 s^{-1}, and f=1.26x10^{-4} s^{-1}; these parameters yield values of B from 1.6 to 6.3. Hence we conclude that the flow regime (B>1) lies well within the blocking regime as noted by Overland & Bond (1995). The literature is full of examples of barrier and coastal jets, the dynamic difference between the two if any, is not distinct. *In this study the term coastal jet (CJ) will be applied to cases where the <u>upstream</u> winds are nearly parallel to the along-barrier axis. A barrier jet (BJ) in turn is applied to cases where the <u>upstream</u> flow is nearly perpendicular to the barrier*. Blocking plays a role in both coastal and barrier jets in that the local pressure gradient is enhanced.

Table 1 list pertinent data on 14 strong E-SE wind cases that have occurred in PWS (primarily at B60) and for which there is sufficient station data for analysis. The typical synoptic pattern for these events is a low center located between Bristol Bay and Kodiak Island (165°-155°W) with a ridge of high pressure located over British Colombia. On occasions, for example during the October 10, 2008 event a triple point low will form in the northwestern Gulf of Alaska and move northward over Cook Inlet or the Kenai Peninsula. Various fronts associated with these low pressure systems migrate northward through the Gulf of Alaska, the majority are occluded fronts with the occasional warm front and rare cold front.
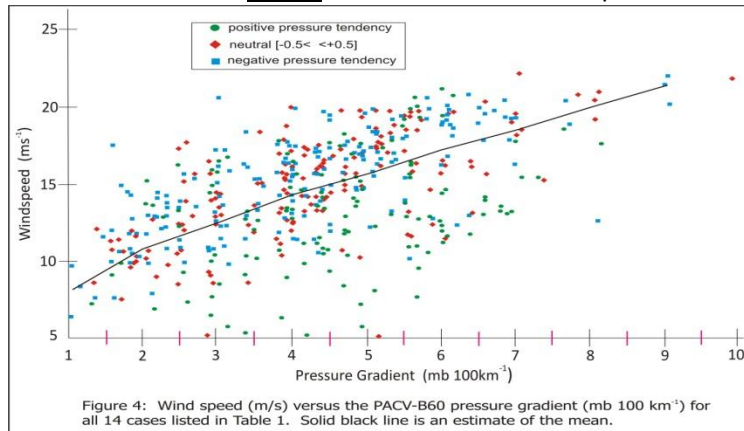
Table 1: *Summary of 14 strong easterly wind events at Buoy 46060. Bold fonts represent statistical significance at 99% confidence level for F-test.*

Date	max wind (m/s)	max gust (m/s)	PACV - B60 (mb/ 100km)	B82 - B60 (mb/ 100km)	2-hr pr. Tendency (mb/2 hr)	Correlation: B60 vs. PACV pr. gradient	Correlation: B60 vs. B82 pr. gradient
March 11, 2005	21.0	28.3	8.1	4.6	-3.0	**+0.73**	**+0.69**
December 7-8, 2005	20.9	28.2	7.7	2.8	-4.8	**+0.57**	+0.34
December 15, 2005	20.4	26.6	6.0	3.5	-1.1	**+0.86**	+0.92
February 5-7, 2006	22.1	29.1	7.1	3.5	-5.5	**+0.62**	+0.36
February 9-11, 2006	22.8	30.0	9.1	4.3	-6.1	**+0.82**	**+0.78**
September 22-23, 2006	21.4	29.1	6.9	3.8	-4.5	**+0.54**	+0.36
October 2-4, 2006	19.6	25.7	6.9	3.2	-3.2	**+0.78**	**+0.58**
October 9-10, 2006	22.1	29.7	9.9	4.9	-6.9	**+0.73**	**+0.67**
December 28, 2006	19.5	26.5	6.5	3.0	-5.8	**+0.85**	**+0.92**
April 7, 2007	20.4	26.2	8.2	4.6	-3.0	**+0.82**	**+0.83**
November 1, 2007	20.4	26.1	6.8	3.0	-2.9	**+0.84**	**+0.67**
November 20-22, 2007	20.6	27.1	6.2	2.9	-1.6	**+0.70**	**+0.56**
October 10-11, 2008	24.1	31.2	4.2	5.5	-4.5	**+0.95**	**+0.85**
January 14-15, 2009	21.1	29.2	6.1	3.2	-4.6	**+0.64**	**+0.63**

From the data displayed in Table 1 several points are noteworthy. First, the PACV-B60 pressure gradient is typically twice as large as is the B82-B60 pressure gradient. One exception is the October 10-11, 2008 case in which the peak pressure gradient was higher along the B82-B60 axis. We speculate that that intense blocking extended further upstream (southeast) than normal.   In general however since PACV is only ~10 km south of the barrier compared to B82 which is ~90 km distant; enhanced blocking by the terrain generates significantly higher MSLP at PACV compared to B82. Second, the 2-hour pressure tendency at B60 varies considerably from one event to the next; however the data indicates that the local pressure is almost always falling markedly around the time of maximum winds. This would seem to support the hypothesis that these winds are related to a synoptic-scale northward moving front. Third, although the coastal pressure gradient dominates, at times the isallobaric component of the wind makes an important contribution (+/-) to the overall speed.

Sustained wind speeds at B60 versus the PACV-B60 pressure gradient is shown in Figure 4. Note how for any given pressure gradient there is a wide range of resulting speeds. The symbols are segregated by the 1-hour pressure tendency at B60. For this type of composite there is little to no grouping of the data. Figure 5 shows pressure gradient versus wind speeds at B60 for the October 10, 2008 event. In this event there is considerable hysteresis (2-hr tendencies) as falling pressures at times

represent higher speeds than rising pressures. This results from fact that the pressure tendencies are measure at discrete points while the actual wind speed results from a larger pressure field.

Figure 4: Wind speed (m/s) versus the PACV-B60 pressure gradient (mb 100 km^{-1}) for all 14 cases listed in Table 1. Solid black line is an estimate of the mean.

Wind gusts at the buoys (5 second averaging) tend to be 20-30% faster than the eight minute sustained winds. Winds at land stations (ASOS), like PACV, tend to display a higher gust to sustained speed ratio then the buoys do, impart due to the shorter averaging period introduced in recent years, and more importantly due to the fact that surface roughness is greater over land than water resulting in strong lower tropospheric turbulence when compared to a large body of water.

During the cooler months it is common for the air temperatures in PWS and along the coast to rise several hours prior to any increase in wind speed or directional change as a resulting of mixing of the boundary layer down to the surface. For the 14 events listed in Table 1, the NARR date set indicates that at the 850 mb level in the northern Gulf of Alaska and PWS eight events displayed moderate-to-strong warm temperature advection, there was one event with moderate-to-strong cold advection (Jan 2009), and five events with minimal temperature advection. For the latter events it is typical for warm advection to occur in the eastern Gulf of Alaska but it does not impact the northern coastal zone.

The near surface thermal properties of many fronts/troughs that move through the northern Gulf of Alaska are frequently diffuse. Air temperatures at the various buoys or C-man stations typically indicate some warming; however a considerable contribution to this warming probably comes from boundary layer mixing. There are clear cases of the passage of a distinct warm or cold front at PAMD and occasionally at B61, but within PWS the fronts/troughs become diffuse the main signature being the pressure minima. January 7, 2001 and October 11, 2008 are good examples where there is a marked decrease in wind speeds at B61 (-10 m/s) and shift in wind direction from E-SE to S-SW. At B60 wind speeds slowly diminish

Figure 5: October 10-11, 2008: Pressure gradient (PACV-B60) versus wind speeds (m/s) at B60.

over the subsequent hours, however there was no change in wind direction and as in the January 7 event, air temperatures cool by 3° C. We attribute the lack of directional change within PWS for most events to the overwhelming strength over the barrier-parallel pressure gradient with respect to the synoptic scale pressure field.
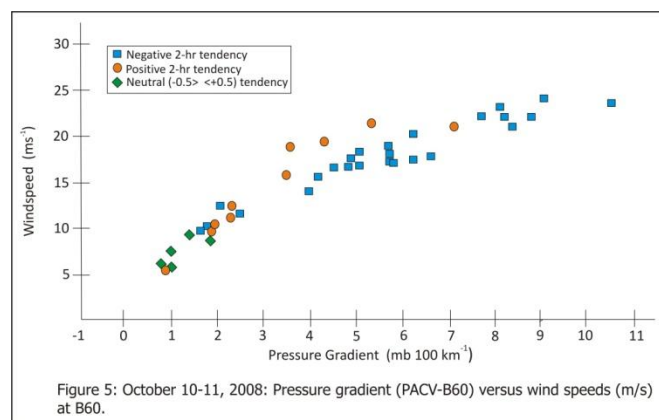
The greatest negative pressure tendencies as seen in the observations tend to occur several hours prior to the passage of the pressure minima which also corresponds to maximum wind speeds.

It is also important to note that pressure tendencies (+-) are greatest in the PWS region then they are further east along the coast- as the former is closer to the low center. The strongest barrier-parallel pressure gradients occur at the time of within several hours of frontal/trough (MSLP minima at B60) passage. MSLP tend to rise and fall at a faster rate and greater range closer to the low center.

It should be noted that B81 and BLIA2 _do not_ have high correlations with upstream pressure gradient because they are influenced by cold air drainage from the Chugach Mountains.   Data from these stations indicate more abrupt changes in speed and direction during the cooler months of the year due to the interplay between cold drainage winds from the north and the warm marine air from the E-SE.   In addition, although B81 and BLIA2 can have periods of strong E-SE winds, the duration of these events is typically shorter than what occurs at B60 and B61.

During periods of peak winds combined sea heights typically range as follows: B82=7-9 m; B61= 7-9 m (max 10.9 m January 19, 2001); B46060= 3-4 m (max of 4.45 m November 9, 1997); B81= 1-1.5 m. Freezing spray can be a problem in northern PWS during periods of cold air drainage, but is generally not a concern during E-SE events. Using the 14 events listed in Table 1, the average wave height at B60 was found to be approximately linear [waveht (m)=0.208*windspeed(m/s)-0.78]. Due to the limited fetch which is on the order of 40-50 km, the response time to changes in wind speed by the waves is on the order of one hour. The highest sea heights at B60 are probably enhanced by swells that pass through Hinchinbrook Entrance and refract in various directions within PWS.

Additional Notable Events: There are a number of events although not listed in Table 1 are of considerable interest. 1) December 21-22, 1999 (see Figure 2) is interesting because even though two fronts move through the area the very strong winds that developed at BLIA2 and Cordova (storm reports of gusts > 53 m/s) were well ahead of the second front; fundamentally due to a very strong pressure gradient that developed as a result of a 1040 mb low positioned over British Columbia and a 984 mb low near western Alaska. Flow in the lower troposphere upstream of the coast was primarily south-southeast. The winds at BLIA2 were some of the strongest recorded for a E-SE event (25 m/s), were on the order of 20-25% higher than at any other station in the region; which is attributed to the blocking that occurred in the immediate vicinity of the barrier.

Event Analysis-February 4-7, 2006:

Observations: Two fronts moved over the northern Gulf of Alaska (at PAMD) during this event, the first at ~20Z Feb 5 and the second at 17Z Feb 6. The first front was associated with a dissipating low which was located in Bristol Bay. A surface analysis drawn by the Ocean Prediction Center shows a weak occluded front at 18Z Feb 5 roughly 150 km south of PAMD while the 00Z Feb 6 chart does not support any fronts north of 54°N. The second front was associated with a low that was developing south of the Alaska Peninsula and had by 06Z Feb 6 moved just south of Kodiak Island at 956 mb (Figure 6). The low center subsequently moved NW into Bristol Bay as it began to dissipate, a similar track as the first low center. The 18Z Feb 6 surface analysis indicates an long occluded front extending from the northern Kenai Peninsula E-SE over PWS and paralleling the coastline all the way to a point just north of Vancouver Island.

Front #1: What is interesting about this particular frontal passage is that there were significant speed decreases at PAMD and B61 at 00Z Feb 6. In the hours preceding frontal passage winds at PAMD and B61 were E-SE with sustained speeds of 20-25 ms^{-1} and gusts ranging from 30-33 ms^{-1}.   As the backside of the front moved through the region (19Z Feb 5 at PAMD) there was however only a modest change in

Figure 6: SAR image for February 6, 2006 12Z with NOGAP wind vectors superimposed.
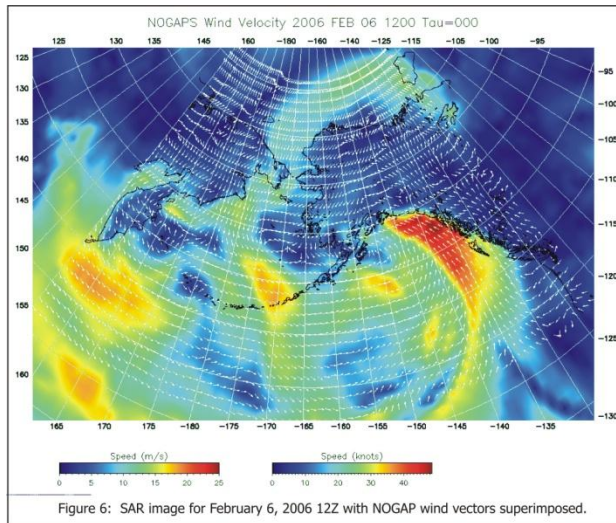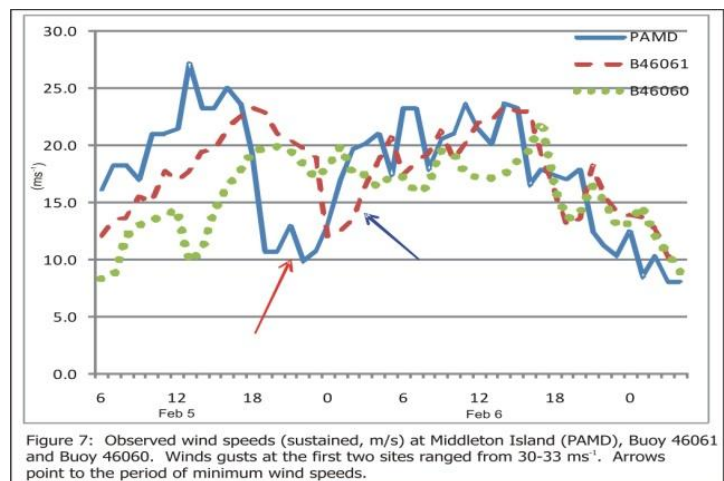
upstream pressure gradient; which leads to the question, why the sharp decrease in speeds? Observations indicate a brief pressure rise early on the Feb 6 (post-frontal) at all PWS stations, as well as at B61 and PAMD; after this brief increase the MSLP field continued another period of sustained decrease (Figure 7). The *pressure gradient* as calculated between PACV and B82 and B61 and B60 only decreased by 1.0-2.0 mb 100 km^{-1}, however during this same period wind speeds at B61 in particular diminished by more than half of their previous values; evidently the decrease in the barrier-parallel pressure gradient was not of sufficient magnitude to account for the large decline in wind speed at B61 and PAMD as well. Wind speeds at B60 and BLIA2 decreased only slightly during this period.

Although far from conclusive it would appear that this was an embedded 'wave' in the synoptic pattern, as indicated by an increase in the MSLP for several hours and then followed by a significant sustained decrease. Closer inspection of the temperature trends at PAMD and B61 indicate that this 'wave' was probably two closely spaced fronts; a warm front during which air temperatures at B61 rose $+5.6^{o}$ C over nine hours, followed by a drop of 2.4^{o} C over the subsequent four hours.

In addition, B76 located 95 km to the east of PAMD experience a sharp rise in air temperatures but no decrease after frontal passage- a possible indication that frontal passage at B76 consisted of a single occluded front. A wedge of higher pressure was sandwiched in between the two fronts. Although air temperatures at B60 and BLIA2 did not show the passage of the cold front, as noted above, pressures did rise slightly during this period. In the postal frontal period wind speeds at PAMD and B61 increased once again (20-23 ms^{-1} with gusts 31 ms^{-1}) until the passage of yet another front (referred to as Front#2) later on Feb 6.

Figure 7: Observed wind speeds (sustained, m/s) at Middleton Island (PAMD), Buoy 46061 and Buoy 46060. Winds gusts at the first two sites ranged from 30-33 ms^{-1}. Arrows point to the period of minimum wind speeds.

Front #2: As noted above E-SE winds re-developed after the passage of the first front and were maintained for some 15-20 hours depending on location. The beginning of frontal passage becomes evident at PAMD at 16Z Feb 6 when the wind direction shifts from 120° to 160° and speeds diminish from 23.2 ms^{-1} to 16.5 ms^{-1}. Wind speeds remain in the teens until 21Z after which they began to ramp down. To the north at B61 the front is first evident at 17Z and 18-19Z at B60. Over PWS air temperatures cooled by 1.5-2.0^{o} C in the several hours prior to the passage of the front. At BLIA2 winds went from NE-E to E-SE and cooled, which is opposite of what one would suspect. Typically the air warms when the winds shift from NE to E at BLIA2 because it indicates the presence of a jet and mixing, while N-NE flow (any speed) represents cold air drainage out of Valdez Arm. MSLP minima occurred from Feb 6, 15Z-17Z and unlike the front on Feb 5, MSLP's rose continuously after frontal passage. The

strongest E-SE winds occurred several hours prior to or during the MSLP minima when the negative pressure tendencies were at their maximum.

WRF model simulation: In order to investigate the dynamics of these events the Weather & Research Forecasting (WRF) model was employed for several events. The model's initial and boundary files utilized the NARR data set. Two grids were used, an outer 12 km grid in order to capture upstream fronts and an inner 3-km. The 3-km grid was sufficient to resolve the majority of terrain details along Alaska's northern gulf coast. The height of the model terrain varies 2,000 m in the Chugach Mountains to 3,000+ m for the St. Elias Mountains. Although this is below the actual heights terrain in the model is sufficient to significantly impede onshore flow. The model was run with full microphysics and boundary layer schemes.

      The simulation for February 5-6, 2006 indicates a slow northward moving front (warm at 900 mb) *with reasonable accuracy when compared to the* sparse observations. The thermal gradient

associated with the front clearly slows down as it approaches the barrier. In addition, near the surface the model does replicate periods of cold air drainage out of Valdez Arm (northern PWS) which verify with the observations, however the model does not generate drainage winds out of the Copper River Delta- which it should have (no observations) considering the magnitude of the arctic airmass that was lying over Alaska at the start of this event. Unfortunately this simulation, which was initialized from NARR data set, only shows a single elevated warm front (Front#1 without its dual nature) throughout the entire simulation period. Model winds along the coast remain strong after the passage of the single front due to the blocked flow. Despite the limitations of the modeling effort it does provide some insight into the evolution of the event.

      As the front moves toward the coastline on Feb 5, in the vicinity of PACV there is from 1° -2° C cooling in a zone 20 km upstream of the base of the barrier concurrent with 2°-4° C warming from 900 mb and above. Cooling is a result of the weak cross-barrier flow attempting to move over the mountain range (the air mass being pushed up-slope). Larger heating over the barrier is evident; some of this heating

Figure 8: Vertical cross-section of total wind speed (m/s) through 145.5° longitude (PACV). A) valid at 06Z February 5 while B) is valid at 16Z February 5. Terrain is blocked out in white.

probably due to the release of latent heat (condensational heating) during the phase transition from water vapor to rain or snow. The concurrent effective MSLP rise in the region underneath the cooling ranges from 0.5-1.5 mb ('effective' because MSLP were decreasing all along the coast, the decrease is less rapid in regions where cooling is taking place). Additionally, a coastal jet begins to form prior to the
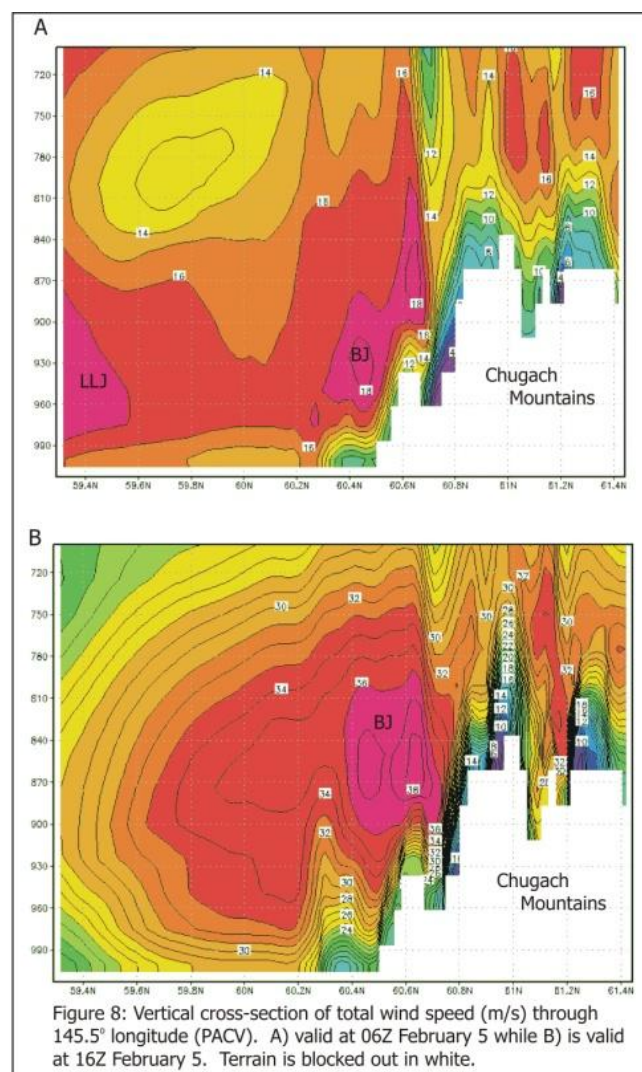
arrival of the frontal LLJ associated in direct response to the aforementioned cooling which was occurring at the base of the barrier. In Figure 8 which is an N-S cross-section of wind speeds, notice that in the top plot (A) a CJ begins to form prior to the arrival of the LLJ which is on the extreme left-hand side (south). Ten hours later the CJ has intensified and moved slightly higher over the barrier. For comparison Olson *et al* (2007) found that the core of coastal jet located adjacent to the Fairweather Range was positioned some 800-1000 m AGL.

The simulated pressure gradient along a north-south transect through 144.3^{o}W increases as the LLJ approaches the coast as seen in Figure 9. The evolution of the lapse rate in the 900-800 mb layer mid-point along this transect is also shown. Initially the correlation is negative but becomes strongly positive as the LLJ moves onshore, this suggests that enhanced stability at the approximate height of the barrier crest plays an important role in the blocking process. The expansion of the cold air dome at the base of the barrier in conjunction with an enhanced N-S coastal pressure gradient <u>initially</u> occurs despite

the fact that there are minimal cross-barrier (~850 mb) winds; the winds in this particular event were nearly parallel to the terrain near the surface but back with height.

Figure 9: North-South pressure gradient (solid line) along 144.3^{o}W and the lapse rate (dashed line) in the 900-800 mb layer mid-point along the transect.
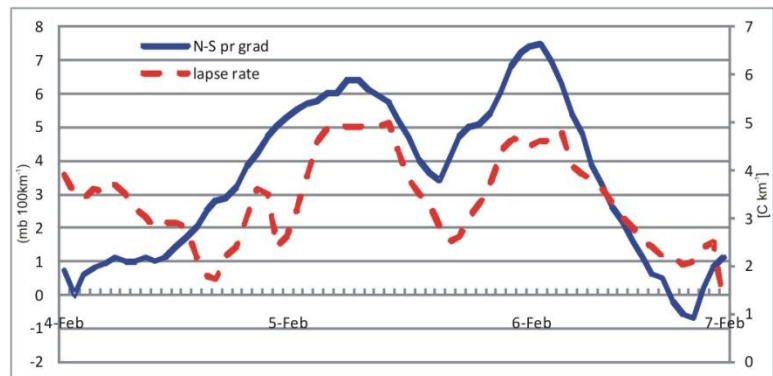
Although not shown in Figure 9, increases in stability typically work from top-down; the 700-800 mb layer lapse rate for example is not only stronger then the 800-900 mb layer, but the former leads the latter in time. In addition, the pressure gradient between this location and PWS closely follows the trend and magnitude (~1 mb higher) of the N-S pressure gradient shown in Figure 9, indicating that as mass is accumulated upstream (SE) along the coast, the barrier-parallel pressure gradient increases in accord with classic barrier jet model.

Upstream blocking is evidence by the upward tilting of the isentropes toward the barrier (not shown). Model precipitation east of PWS ranges from 5 cm along the coast to 25 cm over the highest terrain; most of the precipitation fell on February 6. Storm total observed precipitation was 0.8 cm at Middleton Island and 3.2 cm Cordova airport, how well the model precipitation field over the barrier matches reality can only be a point of speculation since there were no direct observations. This event could be rerun with a dry atmosphere to see the relative importance that phase changes play in the stability of the model atmosphere, as some authors have noted that it may play an important role (Colle *et all* 2002.

Event Analysis- February 9-11, 2006:

Observations: What is of interest with this particular event is the fact that there was an abrupt decrease in east winds at PAMD early on Feb 10 as a warm front moved across the region; there was minimal impact at B61 although the speed decrease at B60 was significant some hours later. All of this occurred while there was N-NE cold air drainage occurring in northern PWS (BLIA2, POTA2). Inspection of NARR files indicate that a LLJ moved into the northern Gulf of Alaska east of 147°W at 18Z Feb 9. By 06Z Feb 10 the LLJ hugged the coast and there was a weak thermal front located in the northern gulf. When this front went through PAMD air temperatures decreased by 2.2^{o} C in an hour (-1.5^{o} C at B76), however at

B61 and B60 air temperatures continued to rise through the period. Although far from conclusive, it would appear that as the front moved on shore it allowed strong N-NE flow to return to PWS as cold air remained in place over Alaska (isobars became more E-W oriented), however the CJ remained intact in a diminished mode (18 m/s) in a narrow band directly south of the barrier as evident by the SE winds at B61 and B82. A second warm front moves through from 20-24Z Feb 10 after which the event concluded.

WRF Simulation: The model handles the first front (warm) correctly with 20-30 m/s low-level winds along the coast. However, no secondary fronts are apparent in the model and more importantly the barrier-parallel winds continue to weaken after the passage of the warm front 0Z Feb 10. This particular effort reinforces the maxima that model output is only as good as the initial/boundary data; overall the model inadequately depicts this event.

Event Analysis- October 9-10, 2008:

Observations: A weak front moves over PWS late on Oct 9 as seen at 900 mb in the NARR data set; however it is not apparent in the surface data. The primary front which generated the strongest winds moved through the northern gulf around 17Z Oct 10. The main points of interest with this event are: 1) Abrupt decrease in wind speeds at B61 between 20Z (21 m/s) and 21Z (5 m/s) as the direction veers from E-SE to S. At B60 meanwhile speeds remained high and there was no change in direction.   2) Strong E winds at BLIA2 (22 m/s) from 20-22Z were coincident with weak north flow in Valdez Arm.

Also, by this time winds at B81 were diminishing and backing to NE due to change in the synoptic pressure pattern. 3) This is a good event to illustrate the variability of frontal passage on wind speed, wind direction, and air temperatures from station-to-station, even though some stations are located very close to each other.   4) Large pressure gradient that forms over the northern Gulf of Alaska late on the Oct 10 is due to the formation of a secondary low over eastern Bristol Bay which subsequently moved NE over the Kenai Peninsula . Meanwhile the high over British Colombia remained quasi-stationary.

WRF model simulation: The model is about three hours too fast on the movement of the front which passes over Middleton Island around 17Z Oct 10; however near surface wind speeds are in relatively good agreement with observations.   It does appear that the winds in PWS and along the coast *near the surface* experience modest accelerations compared to the ambient
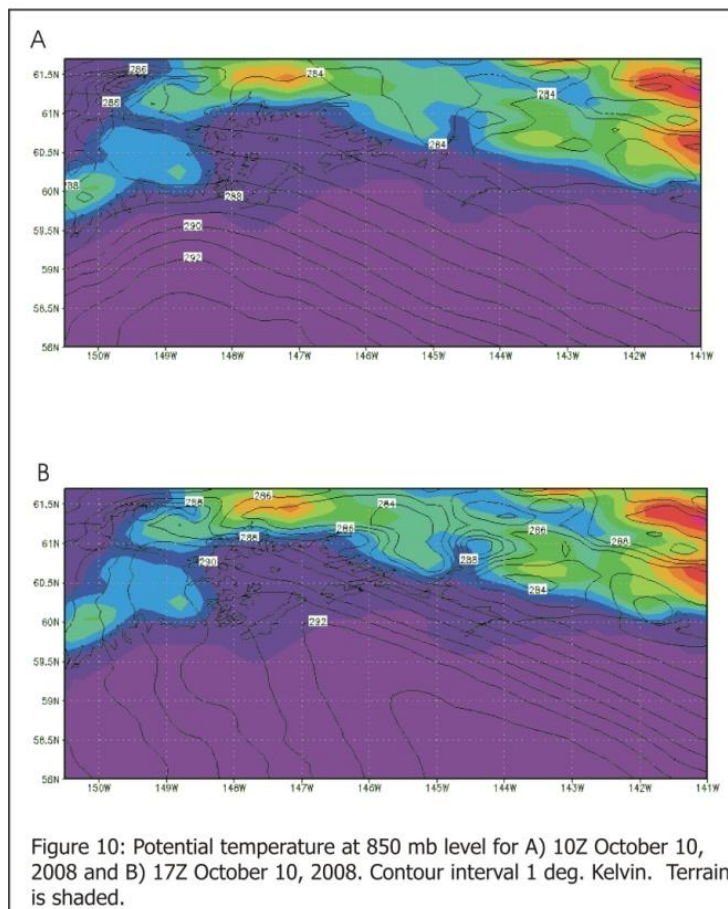

Figure 10: Potential temperature at 850 mb level for A) 10Z October 10, 2008 and B) 17Z October 10, 2008. Contour interval 1 deg. Kelvin. Terrain is shaded.

flow upstream. For example, strongest sustained winds at PAMD are on the order of 18-20 m/s versus 20-24 m/s at stations in PWS.   Vertical cross-sections of model output however shows that when the jet core (950-900 mb) is near the coast there is considerable speed enhancement within the core compared to upstream values.   Upstream core speeds for the LLJ associated with the front, range from 26-30 m/s, significantly weaker then the 40-43 m/s when the jet is located over northern PWS several hours later, similar to Figure 6.

A horizontal plot of frontal contraction at the 850 mb level on Oct 10 is shown in Figure 10. This is attributed to the blocking of lower tropospheric flow over the barrier as it attempts to move toward the NE. In the lower plot notice the cooler air mass to the left which eventually kills the strong wind event.

It should be noted that the model shows minimal difference in wind speeds between the 3-km and 12-km grids in the upstream and near barrier winds (i.e.-max jet cores are within 10%) However, higher details seen on the 3-km grid are a function of the wavelength of terrain variability. Accumulated rain over PWS for entire simulation was 5-10 cm, what impact this had on the vertical temperature profile is unknown.   As the front moves onshore, pressure gradient along the coast increases from 2.2 mb 100^{-1} at 7Z Oct 10 to 4.1 mb 100^{-1} 13Z Oct 10. As noted earlier in this paper the MSLP often decreases throughout the entire region, directly along the coast in areas of intense blocking however the rate at which the pressure decreases is slower than other areas, this heterogeneity of the MSLP field in turns produces large barrier-parallel pressure gradients.

Figure 11 shows two N-S cross-sections of potential temperature on Oct 10. Note the enhanced blocking (slope of isentropes) in the lower plot directly upstream of the barrier. In addition, blocking occurs further upstream (to the left) at higher elevations then it does near the surface in according with the propagation of upstream mountain gravity waves.

Discussion:

1) Although frontal structure can be difficult to asses in detail from the observations, what we do know is that these fronts and associated LLJ not only slow down as they approach the barrier that rings the Gulf of Alaska, but they often stall creating a prolonged period of strong winds. The majority of the cases examined in this paper are associated with some type of LLJ; the orientation of these jets various from barrier-parallel to barrier-perpendicular. Hence there is a fairly wide spectrum of upstream flow parameters that produce strong barrier-parallel winds. These range from NW-SE oriented LLJ which are impeded by the barrier to classic barrier jet conditions (Parish 1982) in which the upstream flow is perpendicular to the barrier and there is a strong pressure gradient across the Gulf of Alaska.

Figure 11: North-South cross-section of potential temperatures (deg Kelvin) through 145.5°W. A) 10Z October 10, 2008; B) 17Z October 10, 2008. C.I.= 0.5° K.

Due to terrain variations both in the coastal zone and along the barrier, as well as the differential advection of fronts, there is considerable variability within the CJ in terms of wind speed.
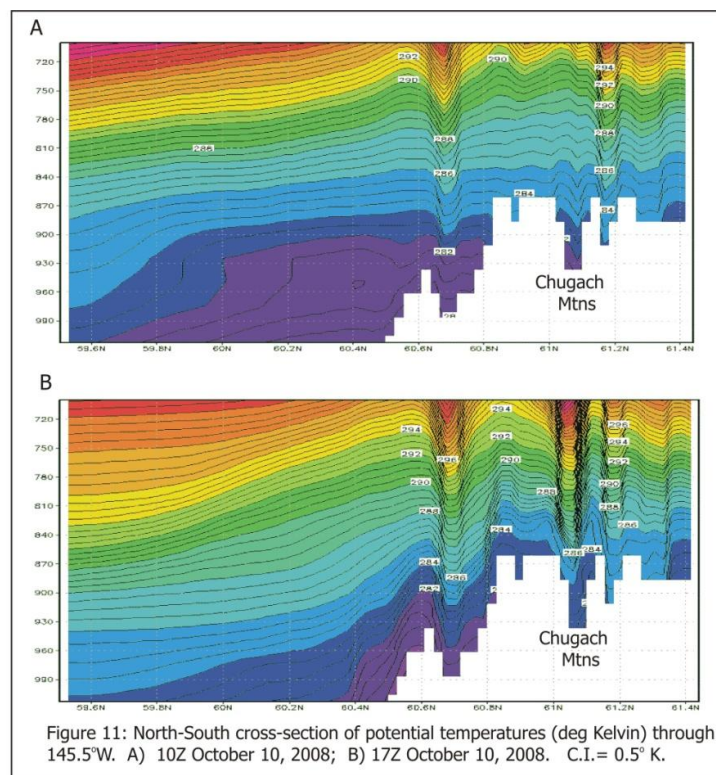
Local terrain (gap, localized barrier) impacts are probably considerable at times. It is difficult to estimate the acceleration within the CJ due to blocking since the application of Overland & Bond (1995) eq.3 is not readily apparent to the current events because the upstream wind speeds are often greater than 15 m/s. Enhancement based on the model is on the order of 15-20 m/s in the elevated CJ core, while wind speeds at the surface are on the order of 10 m/s. As noted above from the surface observations it is difficult to estimate enhancement because speeds at PAMD are frequently similar to those closer to the barrier. This can be due to a number of reasons, two of which are that PAMD may lie within the enhancement zones at times (see next paragraph), and due to the fact that the averaging period for PAMD is considerably shorter (2-min) then for the Buoys or C-Man stations. Low-level aircraft observations would be needed to resolve this issue although based on other studies the enhancement at times is probably considerable.

PAMD which is approximately 160 km downstream of the barrier crest does appear to lie on the edge of the BJ zone. The Rossby radius of deformation which is a measure of the upstream influence that the terrain will have on the blocked flow, is on the order of 120-170 km (L_r=Nh/f; with N~0.01 s^{-1}, h=1500 m, f=1.26x10^{-4}s^{-1}) depending on the value of N used and the height of the barrier that is inserted into the equation. Inspection of the observations as seen in Figure 12 shows that winds at PAMD are as strong as at B61 and stronger than along the coast or in PWS. B61 lies within the CJ zone but at times it is greatly impacted by frontal passage- in other words under certain conditions the wind speed and direction are modified (usually diminished speeds and veering winds) directly by the front. In addition, the
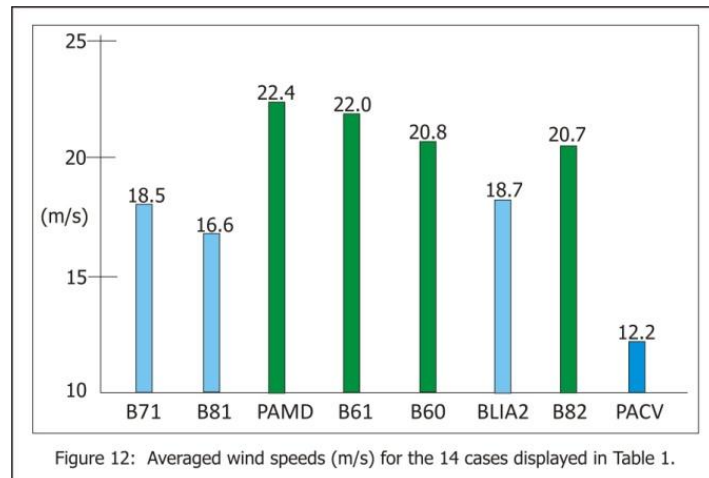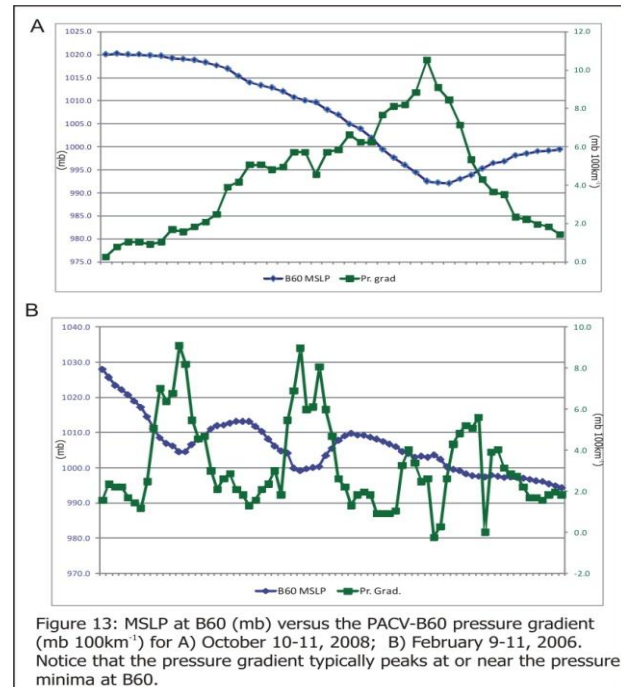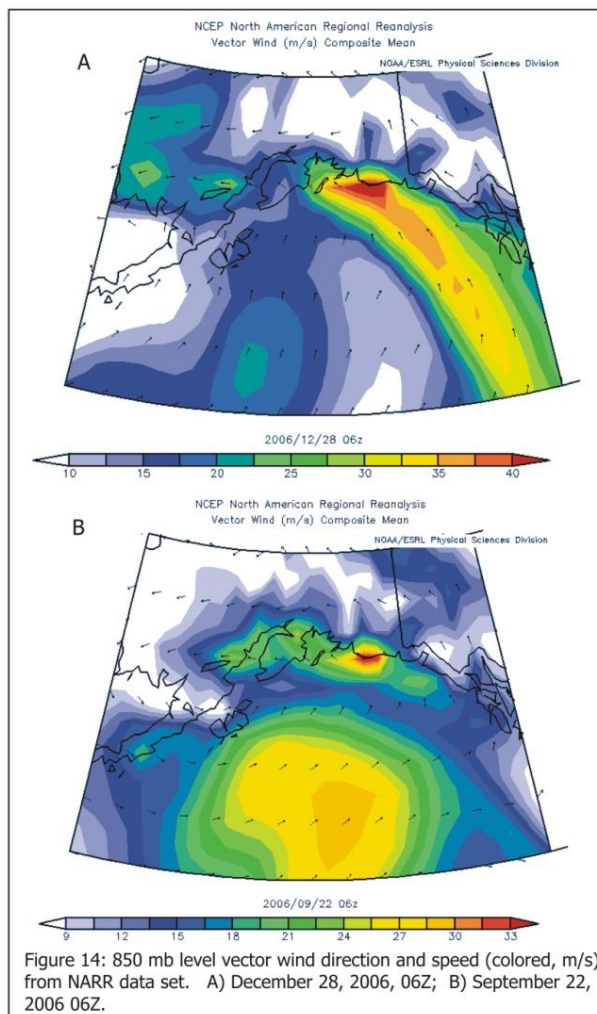

Figure 12: Averaged wind speeds (m/s) for the 14 cases displayed in Table 1.

terrain of Hinchinbrook and Montague Islands under certain conditions enhance wind speeds south of PWS, although during strong E-SE events the enhancement is probably minimal. B60 in contrast is positioned in west Orca Bay and is directly within the BJ zone. In addition, Orca Bay may also provide some enhancement for east winds due to terrain funneling. BLIA2 and B81 by virtue of their location in northern PWS are frequently influenced by drainage winds that flow down the many fjords located in this part of the sound. Observations from these two stations indicate the highly variable nature of the wind direction, speed and air temperatures as drainage winds interact with strong E-SE winds.

The isallobaric component of winds within the CJ zone is difficult to quantify since in these ageostrophic cases one cannot separate the pressure gradient from the pressure gradient tendency since they are interrelated (see Petterssen sec 4.6 for isallobaric analysis). However, qualitative analysis of the observations indicates that the isallobaric component is important at times. Inspection of surface observations clearly indicates that the along coast pressure gradient reaches its maximum value at or near the time of pressure minimum as illustrated by two examples seen in Figure 13. In addition, although only a limited number of cases were simulated using the WRF model, output from the model suggest that blocking is not uniform along the north Gulf Coast; there are preferred areas where blocking tends to be stronger. This would be in part a function of height of the barrier and possibly it's width as well.

In addition, modeling of these events is limited to the quality/resolution of the boundary files which over the North Pacific and Gulf of Alaska in particular, is not as high as it is over most terrestrial regions. This means that modeling efforts at any grid spacing is only as good as the boundary files with respect to fontal resolution.

The sharp southern boundary of jets as seen in SAR imagery (Figures 3 & 6) and discussed by Olson *et all* (2007) and Colle *et al* (2006) would appear to be the demarcation of two different air masses (frontal boundary). NARR indicates a well defined front at 850 mb in the northern Gulf of Alaska for the imagery shown in Figure 3.   Pronounced northern boundaries (some in older imagery may be due to land-ocean masking), especially those in PWS are a result of cold air drainage through the

Figure 13: MSLP at B60 (mb) versus the PACV-B60 pressure gradient (mb 100km⁻¹) for A) October 10-11, 2008; B) February 9-11, 2006. Notice that the pressure gradient typically peaks at or near the pressure minima at B60.
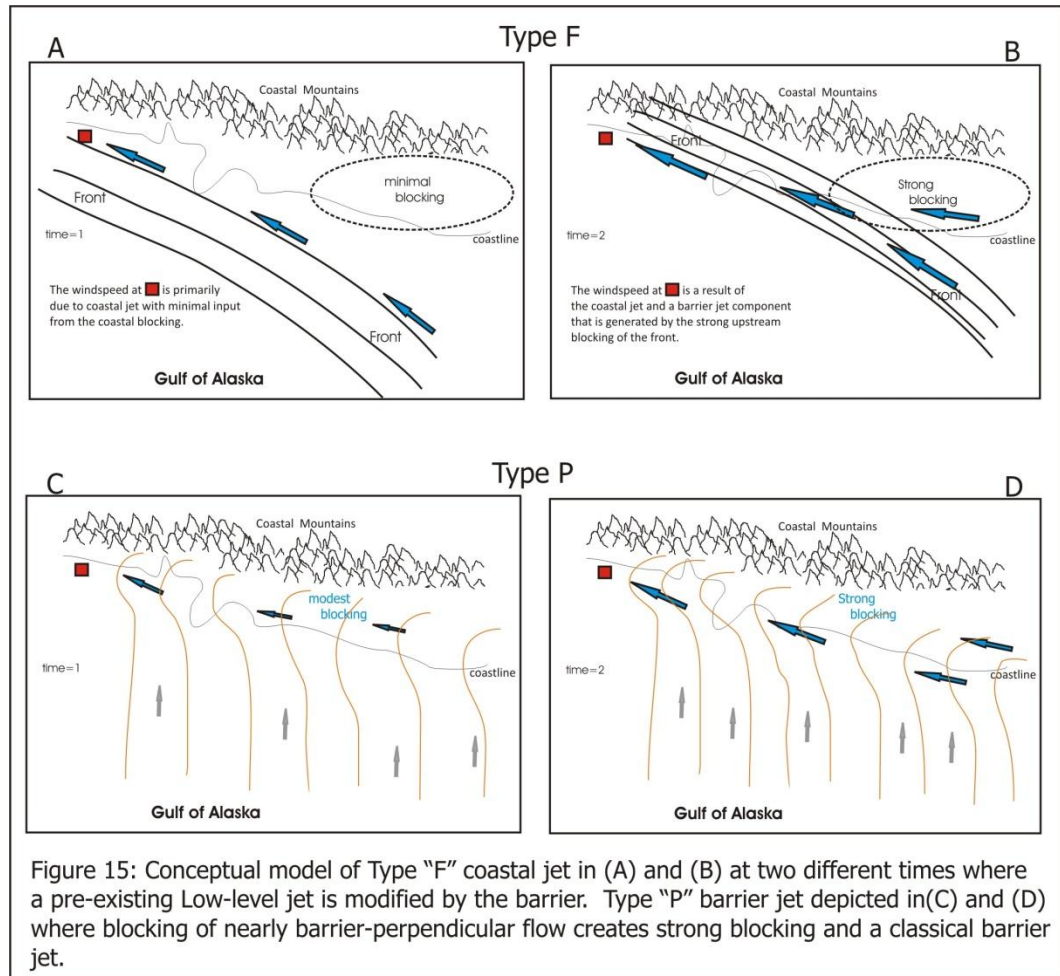
various fjords and bays which in turn limits the northern extension of the coastal jet. In some respects this is equivalent to an arctic frontal boundary separating cold continental air to the north from warmer oceanic air to the south.

Conceptual Model:

The largest MSLP tendencies occur at locations closest to the low center (west), while the dome of high pressure in the east remains stationary. 2) MSLP is a function of the synoptic pressure change as well as any blocking that may occur. Stations closest to the barrier (<50-75 km) have higher MSLP than a station further upstream but would other wise have the same synoptic pressure. 3) LLJ transition to CJ as the air mass is blocked by the barrier. The original jet core stalls just upstream of the barrier and is modified by local blocking. 4) Blocking extends further upstream in the middle troposphere then it does in the lowest 1000 m.

It appears that the strongest E-SE winds along the northern coast of the Gulf of Alaska are closely coupled with fronts and associated LLJ that move northward toward the coastal barrier. There is a broad spectrum of frontal structures that can produce these strong events. Type "F" occurs (Figure 14A, 15A & B) then a front and associated LLJ are oriented roughly barrier-parallel as it moves onshore. The front

Figure 14: 850 mb level vector wind direction and speed (colored, m/s) from NARR data set.   A) December 28, 2006, 06Z; B) September 22, 2006 06Z.

is contracted because it is effectively 'squeezed' between the barrier to the north and the air mass to the south. Once a front becomes blocked the horizontal temperature in the 900-700 mb for example is contracted which produces a stronger thermal wind; this corresponds to the level of the jet core. In addition, warm advection above the boundary layer (occlusion) enhances blocking making it more difficult

Figure 15: Conceptual model of Type "F" coastal jet in (A) and (B) at two different times where a pre-existing Low-level jet is modified by the barrier. Type "P" barrier jet depicted in(C) and (D) where blocking of nearly barrier-perpendicular flow creates strong blocking and a classical barrier jet.
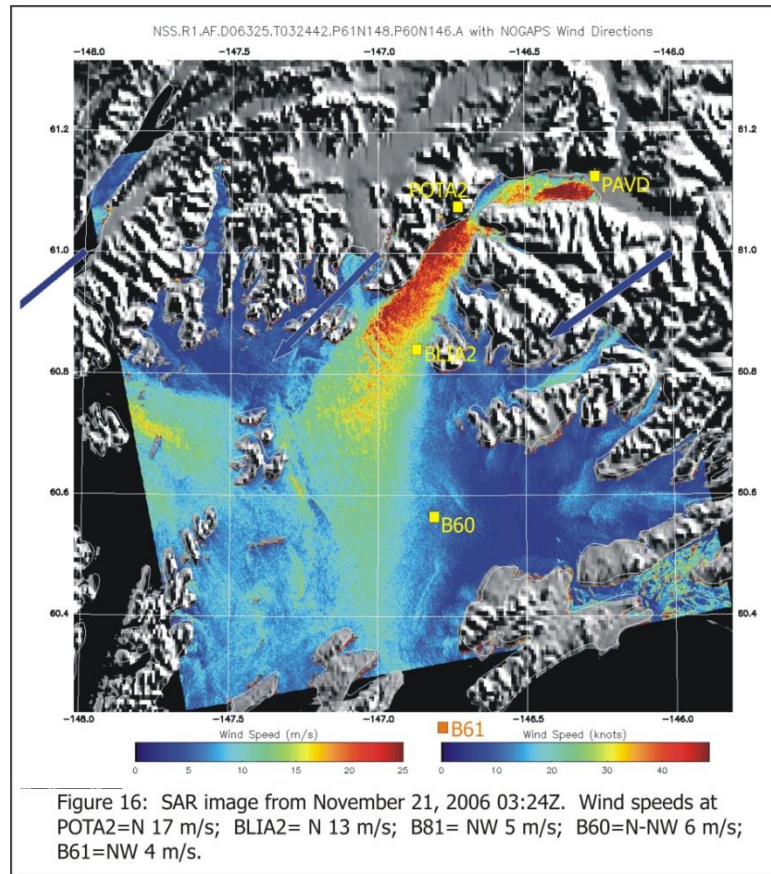
for the front to advance northward over the barrier. It should be noted that as air approaches the barrier there are different rates of temperature change, for example, warm advection may actual produce cooler temperatures near or below barrier crest level due to upslope flow. The important point is that if the lapse rate (stability) decreases (increases) in the lower troposphere blocking will be enhanced. In type "P" the flow upstream of the barrier tends to be southerly or southwesterly (Figure 14B, 15C & D), under these circumstances the onshore flow is blocked and E-SE winds develop due to a very strong barrier-parallel pressure gradient. In type "P" events the front is weaker but is typically present but weaker than type "F" events. Both types have very strong east-to-west MSLP gradients of various orientations. Type "F" tend to be aligned from NW-to-SE while type "P" are more N-to-S or even from NE-to-SW for short periods of time. Type "F" represent pre-existing LLJ's which are modified by the coastal terrain and form coastal jets, while type "P" represent classic barrier jets. In reality, there is considerable blurring of the two types, type "F" may morph into a type "P" in post-frontal situations. The observations also show that a series of fronts may move through the northern Gulf of Alaska in quick success adding to the rich nature of these events.
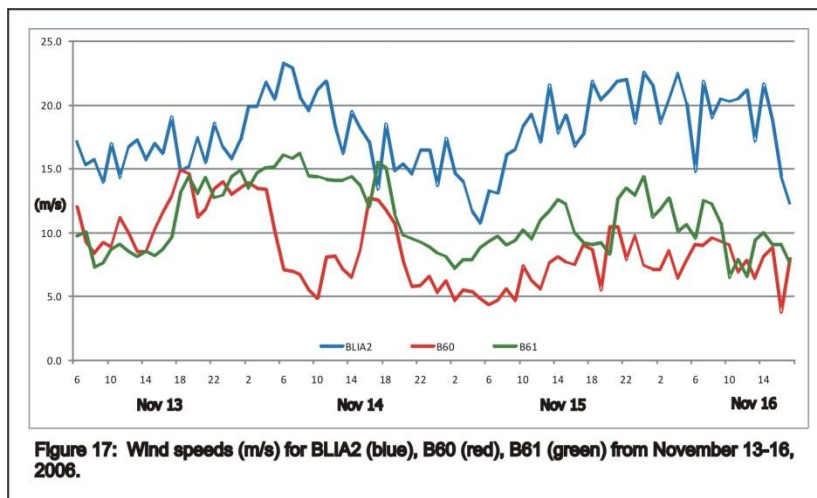
Northerly drainage jets (type "D") are less complex in that cold air moving through gaps in the terrain is accelerated in the classical Bernoulli sense. Further upstream for example in the vicinity of Valdez, drainage these winds are associated with Boras as cold air moves over the higher terrain. Wind speeds can at time reach impressive values even over northern PWS.

North-Northeast Events:

There are typically one to two cold air drainage events per season at BLIA2 in which sustained winds of gale force (>=18 m/s) last for at least several days, although many of these events have a duration of 7 to 10 days. The strongest events can push cold arctic air as far south as B61. Although cold air drainage may be present during strong E-SE wind events as illustrated above, the strongest N cases represent a completely different wind regime. On the synoptic scale high pressure resides over the interior of Alaska or the Yukon with a low center positioned in the eastern Gulf of Alaska. March 12-13, 2003 and November 13-16, 2006 represent two such events; the latter produced moderate to strong N winds throughout the northern PWS through November 28. SAR imagery (Figure 16) indicates that cold air drainage out of Valdez Arm can be characterized as a jet which typically is aimed toward Naked Island (NE-SW trajectory). This type of flow regime will generate strong winds

Figure 16: SAR image from November 21, 2006 03:24Z. Wind speeds at POTA2=N 17 m/s; BLIA2= N 13 m/s; B81= NW 5 m/s; B60=N-NW 6 m/s; B61=NW 4 m/s.

at BLIA2 but only moderate or in some cases weak N to NE winds at B60. Figure 17 shows the sustained wind speeds at BLIA2, B60 and B61 for the November 13-16, 2006 case. Interesting to note that for much of the duration of the event the winds were noticeably stronger at B61 than at B60. For 'typical' drainage flow through a gap we would expect that the speed drops off with distance from the source, in other words winds at BLIA2 should be stronger than at any stations to the south, while winds at B60 should be stronger than at B61. The atypical pattern seen in Figure 17 is probably due to an acceleration

Figure 17: Wind speeds (m/s) for BLIA2 (blue), B60 (red), B61 (green) from November 13-16, 2006.

of the cold air that is being 'pooled' in PWS through Hinchinbrook Entrance. In this case the terrain of Hinchinbrook and Montague Island acts as a gap through which the colder air in the sound is forced to pass through; March 14, 2007 and January 27-31, 1999 are two further examples where the winds at B61 were significantly (200%) stronger than at B60. When the synoptic pattern favors N to NW across PWS (surface low in NE

Gulf of Alaska), then winds at B60 may be on par with those at BLIA2.

Although not displayed in Figure 17, the wind speeds at POTA2 and BLIA2 are or frequently of similar magnitude although it would appear from the two events that were analyzed that they are not necessarily in phase. Both stations at times display considerable short-term (1 hour or less) fluctuations in speeds. Port Valdez with its steep terrain acts as a reservoir for cold air which flows through gaps and passes from the Copper River Basin. This pool of cold air then 'squeezed' through Valdez Narrows into Valdez Arm where it is accelerated. Fluctuations in the depth and temperature of the air within Valdez Arm not only sets the control on the amount of acceleration but is probably responsible for temporal fluctuations in wind speeds at POTA2 and BLIA2. If enough cold air pools within PWS then a secondary acceleration occurs through Hinchinbrook Entrance as well.

Outstanding Questions:

Q1) What impacts do Hinchinbrook and Montague Islands have in isolating PWS from the Gulf of Alaska during E-Se wind events? Can the higher terrain of these islands (700 m) enhance wind speeds at B61? If these islands act as a 'mini barriers' at times, the alignment of pressure gradient would have to be just right. By way of example, at B61 from 05Z-14Z Feb 10 the winds remain strong (18 m/s) but upstream pressure gradients (PACV-B61 ~4.0 mb per 100 km^{-1} and B82-B61 ~1.5 mb per 100 km^{-1}) are relatively weak.

Q2) What contribution to barrier-parallel wind speeds do one to three hour isallobaric tendencies play?

Q3) What is the width of enhanced coastal winds and how does it change with stability, upstream wind direction and frontal passage?

References:

Braun, S.A., R. Rotunno, J.B. Klemp, 1999: Effects of coastal orography on landfalling cold fronts. Part I: Dry, inviscid dynamics. *Jr. Atmos. Sci.*, **56**, 517-533.

Colle, B.A.., B.F. Smull, M-J, Yang, 2002: Numerical simulation of a landfalling cold front observed during COAST: Rapid evolution and responsible mechanisms. *Mon. Wea. Rev*., **130**, 1945-1966.

Colle, B.A., K.A. Loescher, G.S. Young, N.S. Winstead, 2006: Climatology of barrier jets along the Alaskan coast. Part II: Large-scale and sounding composites. *Mon. Wea. Rev*., **134**, 454-477.

Doyle, J.D., 1997: The influence of mesoscale orography on a coastal jet and rainband. *Mon. Wea. Rev*., **125**, 1465-1488.

Li, J., Y-L Chen. 1997: Barrier jets during TAMEX. *Mon. Wea. Rev*., **126**, 959-971.

Loescher, K.A., G.S. Young, B.A. Colle, N.S. Winstead. 2006: Climatology of barrier jets along the Alaskan coast. Part I: Spatial and temporal distributions. *Mon. Wea. Rev*., **134**, 437-453.

Olson, J.B., B.A. Colle, N.A. Bond, N.Winstead. 2007: A comparison of two coastal barrier jet events along the Southeast Alaskan Coast during the SARJET Field Experiment. *Mon. Wea. Rev*., **135**, 2973-2994.

Overland, J.E., N.A. Bond, 1993: The influence of coastal orography: The Yakutat storm. *Mon. Wea. Rev*., **121**, 1388-1397.

Parish, T.R. 1982: Barrier winds along the Sierra Nevada mountains. *J. Appl. Meteor*. **21**., 925-930.

Petterssen, S. 1956. Weather analysis and forecasting. Vol. 1., McGraw-Hill , pp.428.